

RESEARCH PAPER

Cu- Zeolitic Imidazolate Framework-8 Loaded on Magnetic Nanofiber as a High-efficient Antimicrobial Scaffold

Jafar Abdi

Faculty of Chemical and Material Engineering, Shahrood University of Technology, Shahrood, Iran

ARTICLE INFO

Article History:

Received 06 June 2020

Accepted 04 September 2020

Published 01 December 2020

Keywords:

Antibacterial activity;

Chitosan-PVA

Cu-doped ZIF-8

Magnetic nanofiber

Metal organic framework

Nanocomposite

ABSTRACT

In this work, CoFe_2O_4 was synthesized as magnetic agent and blended with chitosan-poly vinyl alcohol (CS-PVA) to fabricate magnetic nanofiber (MNF) by electrospinning method. Zeolitic imidazolate framework-8 (ZIF-8) crystals were used as a porous media to prepare MNF@ZIF-8 nanocomposite. Two different methods were employed for doping copper ions into the MNF@ZIF-8 structure by adsorption and encapsulation procedures. Characterization clarification of as synthesis materials were performed. Mechanical tests showed that magnetic nanoparticles caused to improve tension resistance of CS-PVA nanofibrous scaffold. Antimicrobial tests for the prepared materials were done in against two types of Gram-positive and Gram-negative strains. The inhibition zone diameter values for Cu^{2+} adsorbed-MNF@ZIF-8 (33 mm and 24 mm for *E.coli* and *S.aureus*, respectively) were better than that of Cu^{2+} encapsulated-MNF@ZIF-8 (32 mm and 18 mm for *E.coli* and *S.aureus*, respectively). The obtained results showed that the prepared copper doped MNF@ZIF-8 can be potentially used as a scaffold for further investigations in practical wound healing applications.

How to cite this article

Abdi J. Cu- Zeolitic Imidazolate Framework-8 Loaded on Magnetic Nanofiber as a High-efficient Antimicrobial Scaffold. J Nanostruct, 2020; 10(4): 817-824. DOI: 10.22052/JNS.2020.04.015

INTRODUCTION

In recent years, fabricating of sufficient scaffolds for tissue engineering systems have been attracted great attention. Electrospun nanofibrous composite materials are good candidates to employ in wound healing applications due to their remarkable properties such as high ratio of surface area to volume, dense and interwoven framework, facile surface functionalization, tunable fibers diameter, excellent porosity and high oxygen permeability [1]. Natural or synthetic biomaterials such as chitosan, cellulose, gelatin, collagen, polyurethane, polyethylene are widely used in order to prepare wound dressing [2, 3]. Chitosan (CS) is a natural polysaccharide biopolymer, derived through chitin deacetylation process. Electrospun nanofibers based on CS

have been extremely utilized for wound dressing applications according to the notable advantages including biocompatibility, biodegradability, non-toxicity, antibacterial activity [4, 5]. However, it could be beneficial to improve some disadvantages of the chitosan such as hardly electrospinnable, poor mechanical properties and fast degradation rate by cross-linking and also blending with other synthetic polymers such as poly vinyl alcohol (PVA). PVA is a biocompatible, biodegradable, nontoxic and synthetic water soluble polymer [1].

As a new and attractive porous hybrid materials, Metal-organic frameworks (MOFs) have been widely used in diverse applications including gas storage, molecular sieving, sensors, medical imaging, drug release and heterogeneous catalysis [6, 7]. So far, several researches have been reported the antibacterial activities of

* Corresponding Author Email: Jafar.abdi@shahroodut.ac.ir
Jafar.abdi1989@gmail.com

MOFs and indicated that they exerted bactericidal influences through the liberation of metal cations from the framework into the solution [8]. Zeolitic imidazolate framework-8 (ZIF-8) as subclass of MOFs, has excellent properties such as high specific surface area, tunable channels, as well as good thermal and chemical stability [6]. Moreover, doping some elements such as copper, silver, nickel and etc. with potentially antibacterial activities, is an essential procedure in many wound-healing-related processes. The emergence of nanoscience and nanotechnology in the last decade presents opportunities for exploring the effects of copper nanoparticles in wound healing.

In this work, CoFe_2O_4 was selected as magnetic agent and magnetic chitosan-PVA fiber were successfully fabricated by electrospinning method. Two different methods were applied to synthesis of Cu/ZIF-8. At first method, ZIF-8 crystals initially were coated on magnetic nanofiber and then magnetic CS-PVA-ZIF-8 was placed in copper ion solution to adsorb copper ions. At second method, Cu ions and Zn ions were attributed contemporary in synthesis and Cu ions like Zn ions were placed in crystal structure of ZIF-8 as nodes. The potential application of the prepared scaffolds were examined as antibacterial agents against two kinds of Gram-positive and Gram-negative bacteria. Results illustrated that the synthesized materials had excellent effect on the antibacterial activity, nominating that doping copper ions can act as a beneficial case for future biological perspective.

MATERIAL AND METHODS

The chitosan polymer (deacetylation degree > 93%) was purchased from Solarbio, Ltd. China and the all other utilized materials (iron(III) nitrate, cobalt(II) nitrate, zinc nitrate, copper nitrate, sodium hydroxide (NaOH), PVA, 2-methylimidazole (MIM), acetic acid(70%), ethanol and methanol) in this work were earned from Merck Millipore, Ltd. Germany. Moreover, the antibacterial activities of the prepared materials were evaluated by using two different types of bacterial strains (*Escherichia coli* and *Staphylococcus aureus*). XRD patterns were measured using an X-ray diffractometer (Bruker D8 advanced with $\text{CuK}\alpha$ irradiation of $\lambda = 0.15406$ nm) and the morphology of the structures was investigated using a scanning electron microscopy (SEM, XL30 model) and transmission electron microscopy (TEM, Zeiss-EM10C-100 KV). In order to perform the tensile strength analysis

the nanofibrous mats were cut into 5 mm × 25 mm rectangular strips and their mechanical properties were tested on an electron tensile machine (LLY-006, China) with loading speed of 10 mm/min, distance of 10 mm, break limit of 50% at ambient temperature and humidity of 65%. The magnetic field was determined in a vibrating sample magnetometer (VSM 7400 Lake Shore) at ambient temperature. Inductively coupled plasma optical emissions (ICP-OES) was performed on a Varian 730-OES. The optical density of bacteria suspension was detected at 600 nm applying a UV spectrophotometer for determination of bacterial turbidity.

Synthesis of magnetic nanoparticle

CoFe_2O_4 nanoparticles (CFO NPs) were synthesized according to the described procedure by D. Moitra [9] using co-precipitation method. Briefly, 4 g of $\text{Fe}(\text{NO}_3)_3 \cdot 9\text{H}_2\text{O}$ and 1.5 g of $\text{Co}(\text{NO}_3)_2 \cdot 6\text{H}_2\text{O}$ were sonicated in 20 mL of double distilled water for 30 min. Next, the mixture solution was added dropwise to NaOH solution (1 M) for adjusting pH followed by stirring for 3 h under N_2 bubbling. Then, the final mixture was refluxed at 120 °C for 12 h. After the completion of reaction process, the precipitated particles were washed several times using double distilled water, ethanol and acetone for several times. Then the particles were dried in a vacuum oven at 80 °C for 24 h to get the final product. Finally, the obtained particles were calcined on alumina crucible at 600 °C for 3 h with a heating rate of 10 °C/min in order to improve the crystallinity.

Electrospinning of CS-PVA and CFO/CS-PVA nanofiber

0.7 g PVA and 0.7 g CS (7 wt.%) were separately dissolved in 9.5 mL of acetic acid (70%) and mixed by magnetic stirring at 50 °C to get a clear solution. After that, chitosan was added to PVA solution with the ratio of 1:4 and the final solution was mixed for 24 h at 50 °C until a homogenous honey yellow solution obtained. For the last step, the solution was sonicated to remove the bubbles for 5 minutes. Then a 5 mL plastic syringe with a needle diameter of 0.4 mm was filled with CS-PVA homogenous polymeric solution. The electrospinning machine ejected the spinning solution by a syringe pump at a constant flow rate of 1 mL/h toward a rotating drum (120 rpm) placed 100 mm apart. The electric field (19kV) was applied from a high

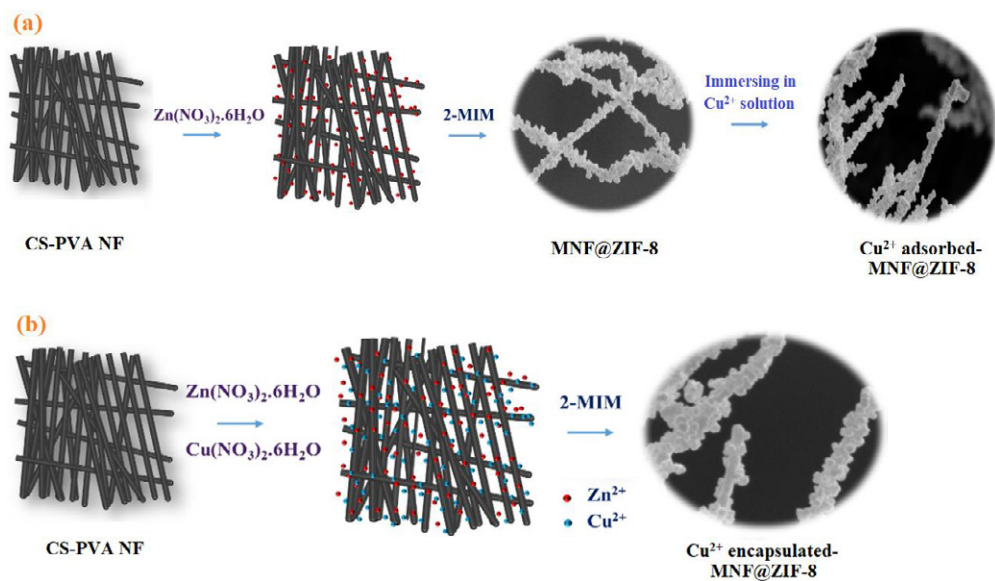


Fig. 1. Schematic illustration of the synthesis procedure: a) Cu^{2+} adsorbed-MNF@ZIF-8 and (b) Cu^{2+} encapsulated-MNF@ZIF-8.

voltage supply source. Synthesis of CFO/CS-PVA was performed by adding CFO NPs to the CS-PVA cross-linked solution and mixing for 24 h to reach a well-dispersed homogeneous mixture. Fabrication process of the CFO/CS-PVA was done exactly in same way of CS-PVA.

Synthesis of Cu adsorbed and Cu encapsulated-magnetic fiber@ZIF-8

ZIF-8 crystals were successfully coated on the surface of CFO/CS/PVA using several cycles at room temperature. ZIF-8 precursor containing 0.587 g of zinc nitrate was sonicated for an hour, followed by mixing with 0.2 g of CFO/CS-PVA nanofiber sheets for 2 h. Then, concentrated 2-methylimidazole (MIM) solution (1.3 g/40 mL) was added to former solution drop by drop under stirring. Then the mixture was maintained in room condition for 24 h to let ZIF-8 nuclei grow up. Synthesized CFO/CS-PVA/ZIF-8 magnetic nanofiber (MNF@ZIF-8) was separated from solution using an external magnet before drying in a vacuum oven at 80 °C for 12 h and washing several times by methanol. The prepared MNF@ZIF-8 was placed in copper nitrate solution with high concentration and stirred to adsorb Cu ions into the porous media. After 2 h the fibers were separated and put in 60 °C oven for 12 h and called Cu^{2+} adsorbed-MNF@ZIF-8. In synthesis of Cu^{2+} encapsulated-MNF@ZIF-8, copper nitrate hexahydrate were companied zinc nitrate with equal molar ratio under N_2 flow

in 40 ml of methanol with 0.2 g of MNF. The rest of synthesis was same as the above-mentioned procedure for Cu^{2+} adsorbed-MNF@ZIF-8.

Study of antibacterial activity

Assessment of antibacterial activity was performed to impede the growth of *Escherichia coli* (*E. coli*, ATCC 1105) and *Staphylococcus aureus* (*S. aureus*, BBRC 10050) bacteria using agar plate disk diffusion method [10]. Primarily, all glassware and samples were maintained in autoclave at 120 °C for a period of 30 min for complete sterilization. Then, nutrient agar culture media was sterilized and poured into the separated sterile petri dishes. Afterward, inoculation was accomplished via transferring 100 μL of each bacteria suspension into the plates followed by dissipating uniformly. The inoculated agar surface was straightly put in touch with 3 mg of nanostructured materials and then plates were incubated at 37 °C for 24 h and finally, the inhibition zones were measured. The minimum inhibitory concentration (MIC) and minimum bactericidal concentration (MBC) were also determined using the microdilution technique as reported in our previous work [10]. The experiments were performed in triplicate and repeated three times.

RESULTS AND DISCUSSION

Imaging analysis was carried out to evaluate morphology, particle size and the shape of

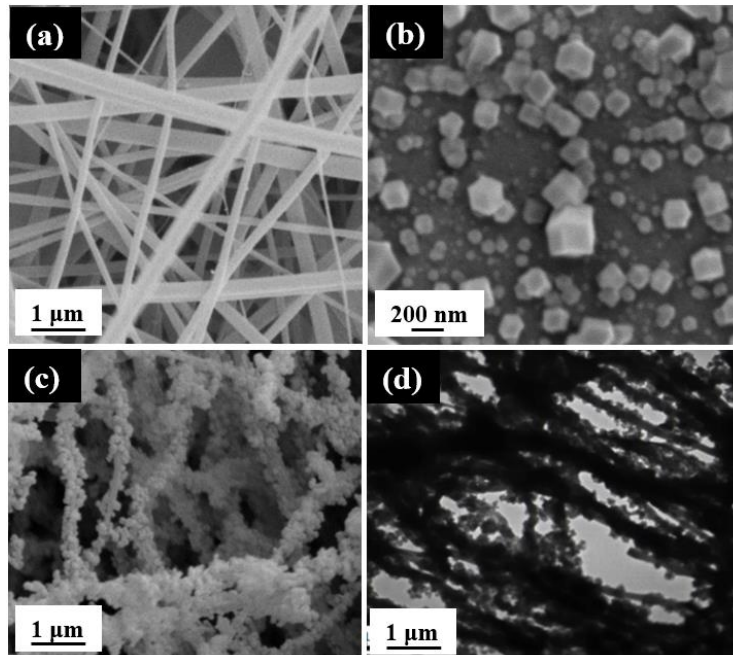


Fig.2. SEM images of (a) CS-PVA NF, (b) pure ZIF-8 NP, (c) Cu²⁺ adsorbed-MNF@ZIF-8 and (d) TEM image of Cu²⁺ adsorbed-MNF@ZIF-8.

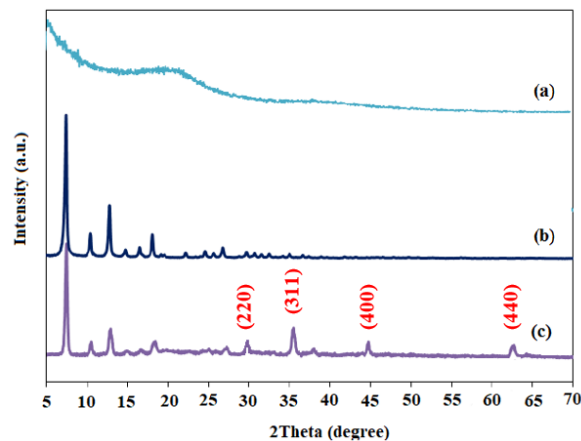


Fig. 3. XRD pattern of materials: (a) CS-PVA NF, (b) pure ZIF-8 NP, (c) Cu²⁺ adsorbed-MNF@ZIF-8.

synthesized materials, by means of scanning electron microscopy (SEM). As illustrated in Fig. 2a, the CS/PVA nanofibers are successfully fabricated with the narrow size of diameters less than 100 nm, without any agglomeration. The prepared nanofibers showed smooth and no defects in morphology. In Fig.2b, ZIF-8 particles illustrate non-uniform size in the range of 100-600 nm since many factors can affect the nucleation process and formation of the crystals. The shape of ZIF-8 particles conforms to the other reports for morphological structure in the literature [11-13].

It is clear from Fig. 2c that the ZIF-8 crystals have been grown onto the nanofiber surfaces uniformly. In addition, the transmission electron microscopy (TEM) was used for further investigation of Cu²⁺ adsorbed-MNF@ZIF-8 structure. Indeed, the pearl necklace shape was perfectly observed from the final product of copper doped MNF@ZIF-8.

XRD analysis were employed to evaluate the crystallinity of the pure and Cu-doped ZIF-8 structures as shown in Fig. 3. The synthesized ZIF-8 pattern is similar to the other ZIF-8 samples reported in the literature [14, 15]. The well-

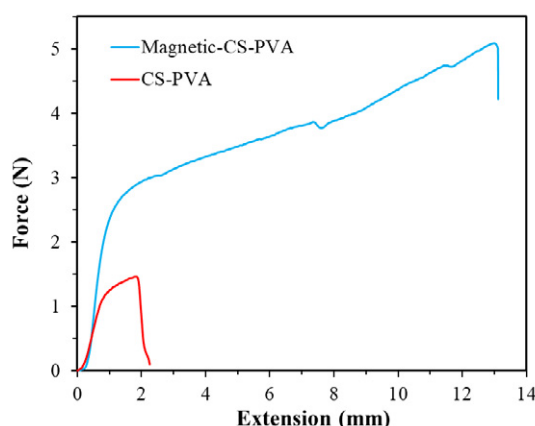


Fig. 4. Mechanical resistance test for the prepared nanofibers.

defined and intense peaks at 2θ values of 7.37° , 10.40° , 12.73° , 14.69° , 16.45° , 18.03° , 22.12° , 24.49° , 25.7° , 26.65° , 29.9° , 30.85° , 31.76° and 32.51° revealed a high crystallinity of the sodalite (SOD)-type ZIF-8, relating to the diffraction planes of 011, 002, 112, 022, 013, 222, 114, 233, 224, 134, 044, 334, 244 and 235 [16]. The obtained data for the copper doped-MNF@ZIF-8 indicated that the intensity of composite peaks were more feeble than that of the pure ZIF-8. In fact the presence of the nanofiber in the framework of the composite, caused the low-intensity peaks in the XRD pattern which is attributed to the hydrogen bonding between components of fiber [17, 18]. In addition, the XRD planes (220), (311), (400) and (440) are well matched with the standard JCPDS data of CoFe_2O_4 magnetic nanoparticles (card no.: 22-1086) [19] appeared in Cu^{2+} adsorbed-MNF@ZIF-8 pattern.

ICP-OES analysis was accomplished to determine the composition of Co, Fe, Zn, and Cu elements in the structure of copper-doped magnetic nanofibers. According to this analysis, each gram of Cu^{2+} adsorbed-MNF@ZIF-8 sample contained 10.3% Co, 12.8% Fe, 16.3% Zn, and 2.58% Cu. Also, each gram of Cu^{2+} encapsulated-MNF@ZIF-8 sample contained 11.1% Co, 11.9% Fe, 17.3% Zn, and 1.97% Cu.

In order to examine the extension resistance of the prepared nanofibrous scaffolds, they were tested by tensile strain analysis. As can be seen from the tensile strength diagram in Fig. 4, pure CS-PVA nanofiber showed weak resistance against extension force. But adding magnetic cobalt ferrite nanoparticles, improved the tensile resistance up to 13.1 mm under 5.2 N extension force. This

proposes that magnetic nanofiber can be stable enough against rupture which is essential property for wound healing textures.

The magnetic properties of cobalt ferrite nanoparticles, magnetic-CS-PVA nanofiber and Cu^{2+} adsorbed-MNF@ZIF-8 are displayed in Fig. 5. The apparent difference between the two patterns showed that magnetic-CS-PVA had smaller magnetization saturation (M_s) value (34.8 emu/g) than the CoFe_2O_4 particles (64.2 emu/g). This difference is related to polymeric CS-PVA nanofibers with dielectric property. After coating magnetic nanofibers with ZIF-8 crystals and Cu^{2+} ions, the magnetization saturation (M_s) value of Cu^{2+} adsorbed-MNF@ZIF-8 decreased to 21.8 emu/g, but it still has strong magnetization showing this nanocomposite is appropriate for the purpose of magnetic separation and recovery.

Antibacterial activity

In order to evaluate the antibacterial activity of the prepared materials, the inhibition zone was measured appeared on agar plates under visible-light irradiation. The MNF@ZIF-8, Cu^{2+} encapsulated-MNF@ZIF-8 and Cu^{2+} adsorbed-MNF@ZIF-8 were investigated and compared with each other against killing both *E.coli* and *S. aureus* strains as shown in Fig. 6. The maximum amount of inhibition zone diameters for MNF@ZIF-8 were obtained 13 and 9 mm for *E.coli* and *S.aureus*, respectively. In our previous work [10], the pure ZIF-8 showed good enough performance (10.8 and 14.8 mm for *E.coli* and *S.aureus*, respectively) which confirms the capability of zinc ions against bacterial cell. In order to investigate two different procedures for doping copper ions,

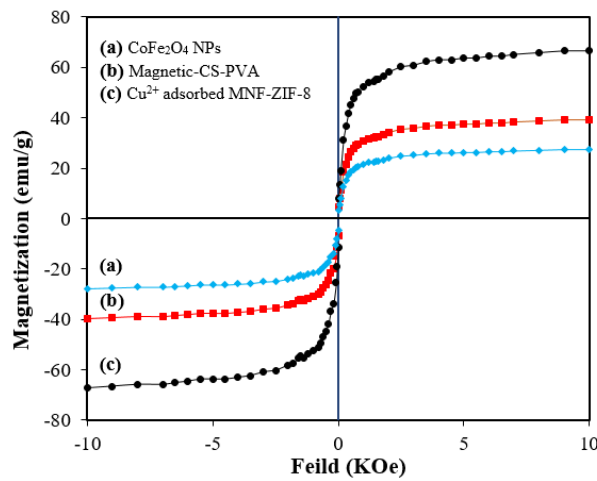


Fig. 5. Magnetization curve of the prepared materials at room temperature.

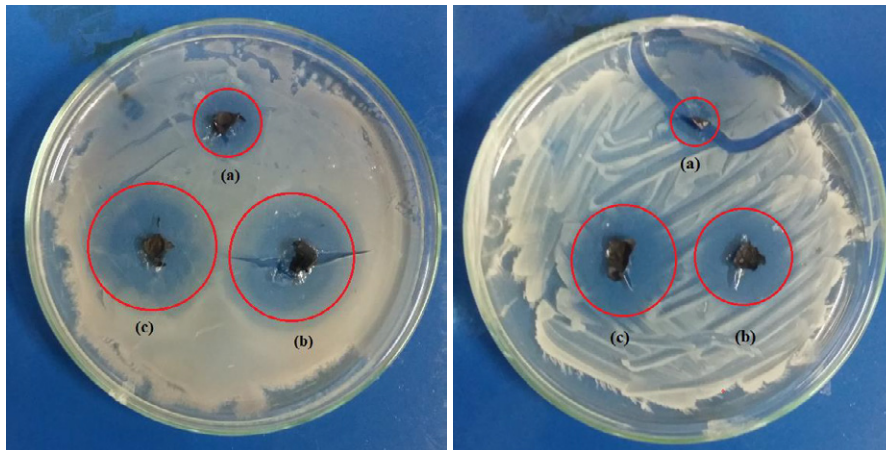


Fig. 6. The digital photographs showing the antibacterial activity of (a) MNF@ZIF-8, (b) Cu²⁺ encapsulated-MNF@ZIF-8 and (c) Cu²⁺ adsorbed-MNF@ZIF-8 against Escherichia coli (left) and Staphylococcus aureus (right) bacteria.

Cu²⁺ encapsulated-MNF@ZIF-8 and Cu²⁺ adsorbed-MNF@ZIF-8 were evaluated for their antibacterial activities. The inhibition zone diameter values for Cu²⁺ adsorbed-MNF@ZIF-8 were better than that of Cu²⁺ encapsulated-MNF@ZIF-8 (Table 1). This illustrates that adsorbed copper ions can be released easily, even though the copper encapsulated sample had excellent efficiency for killing both Gram-positive and Gram-negative bacteria. Different mechanisms have been reported which belong to the copper NPs role affecting as antibacterial agent [20]. It has been found that copper NPs cause several toxic impacts including production of reactive oxygen species (ROS), lipid peroxidation, DNA degradation and protein oxidation. Also, these NPs can be affect

through formation of reactive complex with cellular medium organics. In addition, it should be emphasized that released Cu²⁺ ions from the NPs can be more effective than the primarily present Cu ions in the precursor solution [20]. The obtained results showed that the prepared copper doped MNF@ZIF-8 can be potentially used as a scaffold for further investigations in practical wound healing applications. The results indicated that MIC and MBC test have the same trend so that *S. aureus* with lower zone inhibition diameters have higher MIC and MBC values (Table 2).

In order to investigate the quantity of Cu ions in the solution during the growth inhibition test, an additional experiment was performed to calculate the amount of released copper ions

Table 1. The inhibition zone diameters for all prepared materials against *E.coli* and *S.aureus* bacteria.

Material	Zone of inhibition (mm)		References
	<i>E.coli</i>	<i>S.aureus</i>	
MNF@ZIF-8	13	9	
Cu ²⁺ encapsulated-MNF@ZIF-8	32	18	This work
Cu ²⁺ adsorbed-MNF@ZIF-8	33	24	
Chitosan/PEO/thyme nanofiber	0	39	(21)
Fe ₂ O ₃ @SiO ₂ @ZIF-8-Ag	26.4	25.6	(10)
<i>Lippia citriodora</i> leaf	21	15	(22)
<i>Ficus sycomorus</i> leaf	14	9	(23)
GO/Ag NPs	11.3	15.2	(24)
GO/CuO NPs	12.5	17.3	(24)
CA/PCL fibrous	2.4	2.9	(25)
ZnO@CA/PCL	8.2	9.2	(25)
AgO@CA/PCL	11	12.1	(25)
CuO@CA/PCL	10	9.4	(25)

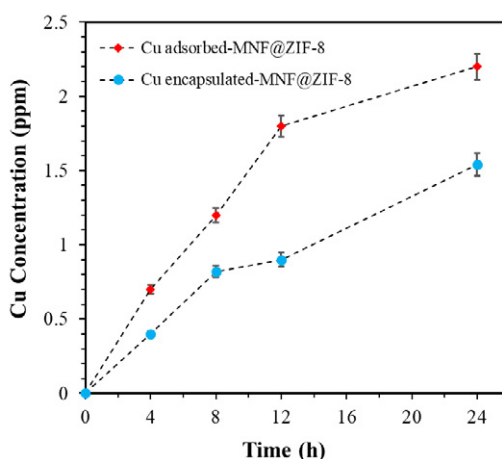


Fig. 7. Concentration of Cu²⁺ released in the experiment environment.

Table 2. MIC and MBC results for Bacteria

Compound	Bacteria	MIC (µg.ml ⁻¹)	MBC (µg.ml ⁻¹)
Cu ²⁺ encapsulated-MNF@ZIF-8	<i>E.coli</i>	152	289
	<i>S.aureus</i>	322	439
Cu ²⁺ adsorbed-MNF@ZIF-8	<i>E.coli</i>	141	255
	<i>S.aureus</i>	301	399

tracked by ICP-OES analysis versus time. The result of elemental analysis showed that 2.58% of the sample contained Cu ions. Additionally, it could be concluded from the findings in Fig. 7 that about 84% and 78% of copper ions existing in 10 mg of Cu²⁺ adsorbed-MNF@ZIF-8 and Cu²⁺ encapsulated-MNF@ZIF-8 were released after 24 h, respectively. Therefore, this high amount of released copper ions is responsible for inhibiting the growth of bacteria in the solutions.

CONCLUSIONS

In summary, porous MNF@ZIF-8 was successfully synthesized at room temperature and two different ways were employed for installation of copper NPs in MNF@MOF structure. The pearl necklace shape was perfectly observed from the final product of copper doped MNF@ZIF-8 with the high crystallinity. Magnetic nanoparticles enhanced the mechanical tension resistance of CS-PVA nanofibrous scaffold. The results

demonstrated that the prepared nanocomposite had good stability and also could considerably inhibit from the growth of both *E.coli* and *S. aureus* strains. Cu²⁺ adsorbed-MNF@ZIF-8 showed the best performance with the inhibition zone diameters of 33 mm and 24 mm, for *E.coli* and *S. aureus* respectively, due to the facile liberation from the MNF@ZIF-8 framework. Therefore, the proposed bio-synthesized material can be considered as excellent candidates for a wide range of biological intentions.

ACKNOWLEDGMENTS

The present work was accomplished in faculty of chemical and materials engineering, Shahrood University of Technology.

CONFLICT OF INTEREST

The authors declare that there is no conflict of interests regarding the publication of this manuscript.

REFERENCES

1. Abdi J, Abedini H. MOF-based polymeric nanocomposite beads as an efficient adsorbent for wastewater treatment in batch and continuous systems: Modelling and experiment. *Chemical Engineering Journal*. 2020;400:125862.
2. Abdi J, Vossoughi M, Mahmoodi NM, Alemzadeh I. Synthesis of metal-organic framework hybrid nanocomposites based on GO and CNT with high adsorption capacity for dye removal. *Chemical Engineering Journal*. 2017;326:1145-58.
3. Abdi J, Vossoughi M, Mahmoodi NM, Alemzadeh I. Synthesis of amine-modified zeolitic imidazolate framework-8, ultrasound-assisted dye removal and modeling. *Ultrasonics Sonochemistry*. 2017;39:550-64.
4. Adeli H, Khorasani MT, Parvazinia M. Wound dressing based on electrospun PVA/chitosan/starch nanofibrous mats: Fabrication, antibacterial and cytocompatibility evaluation and in vitro healing assay. *International Journal of Biological Macromolecules*. 2019;122:238-54.
5. Karimi Alavijeh R, Beheshti S, Akhbari K, Morsali A. Investigation of reasons for metal-organic framework's antibacterial activities. *Polyhedron*. 2018;156:257-78.
6. Bakshi PS, Selvakumar D, Kadirvelu K, Kumar NS. Chitosan as an environment friendly biomaterial – a review on recent modifications and applications. *International Journal of Biological Macromolecules*. 2020;150:1072-83.
7. Chatterjee AK, Chakraborty R, Basu T. Mechanism of antibacterial activity of copper nanoparticles. *Nanotechnology*. 2014;25(13):135101.
8. Gualino M, Roques N, Brandès S, Arurault L, Sutter J-P. From ZIF-8@Al₂O₃ Composites to Self-Supported ZIF-8 One-Dimensional Superstructures. *Crystal Growth & Design*. 2015;15(8):3552-5.
9. Hoffman AS. Hydrogels for biomedical applications. *Advanced Drug Delivery Reviews*. 2012;64:18-23.
10. Islam A, Yasin T, Rafiq MA, Shah TH, Sabir A, Khan SM, et al. In-situ crosslinked nanofiber mats of chitosan/poly(vinyl alcohol) blend: Fabrication, characterization and MTT assay with cancerous bone cells. *Fibers and Polymers*. 2015;16(9):1853-60.
11. Li Y, Jin Z, Zhao T. Performance of ZIF-67 – Derived fold polyhedrons for enhanced photocatalytic hydrogen evolution. *Chemical Engineering Journal*. 2020; 382: 123051.
12. Lin K-YA, Chang H-A. Zeolitic Imidazole Framework-67 (ZIF-67) as a heterogeneous catalyst to activate peroxymonosulfate for degradation of Rhodamine B in water. *Journal of the Taiwan Institute of Chemical Engineers*. 2015;53:40-5.
13. Mahmoodi NM, Abdi J. Surface Modified Cobalt Ferrite Nanoparticles with Cationic Surfactant: Synthesis, Multicomponent Dye Removal Modeling and Selectivity Analysis. *Progress in Color, Colorants and Coatings*. 2019;12(3):163-177.
14. Moitra D, Hazra S, Ghosh BK, Jani RK, Patra MK, Vadara SR, et al. A facile low temperature method for the synthesis of CoFe₂O₄ nanoparticles possessing excellent microwave absorption properties. *RSC Advances*. 2015;5(63):51130-4.
15. Ovington LG. Advances in wound dressings. *Clinics in Dermatology*. 2007;25(1):33-8.
16. Rabea EI, Badawy MET, Stevens CV, Smagge G, Steurbaut W. Chitosan as Antimicrobial Agent: Applications and Mode of Action. *Biomacromolecules*. 2003;4(6):1457-65.
17. Rahmati Z, Abdi J, Vossoughi M, Alemzadeh I. Ag-doped magnetic metal organic framework as a novel nanostructured material for highly efficient antibacterial activity. *Environmental Research*. 2020;188:109555.
18. Son Y-R, Ryu SG, Kim HS. Rapid adsorption and removal of sulfur mustard with zeolitic imidazolate frameworks ZIF-8 and ZIF-67. *Microporous and Mesoporous Materials*. 2020;293:109819.
19. Song Z, Wu Y, Cao Q, Wang H, Wang X, Han H. pH-Responsive, Light-Triggered on-Demand Antibiotic Release from Functional Metal-Organic Framework for Bacterial Infection Combination Therapy. *Advanced Functional Materials*. 2018;28(23):1800011.
20. Yang Q, Ren S, Zhao Q, Lu R, Hang C, Chen Z, et al. Selective separation of methyl orange from water using magnetic ZIF-67 composites. *Chemical Engineering Journal*. 2018;333:49-57.